Phillips University Marburg

Chemical Biology Practical Course CB1-PR

Summer semester 2023

FINAL REPORT OF THE CB1-PRACTICAL COURSE

SS23

submitted by

Matriculation number:

Master Chemistry

Box 2, Table 19

Assistants: Valeska Viereckt and Van Tuan (Marco) Trinh (AG VÁZQUEZ)

Index:

1. Abbreviation.....1
2. Introduction.....4
   2.1 Chemical biological theories.....4
      2.1.1 Introduction to fluorophore and biomolecule dyes.....4
      2.1.2 Solid phase peptide synthesis & antimicrobial peptide.....7
      2.1.3 Bioassay – Hemmhof test and bacteria's growth curve.....10
   2.2 Task summary.....11
3. Result.....11
   3.1 Organic synthesis of Fluorescein.....12
   3.2 Solid phase peptide synthesis.....13
   3.3 Bioassay - Hemmhof.....16
   3.4 Bioassay – Growth Curve.....17
4. Discussion.....20
5. References.....21
6. Attachment.....23

1. Abbreviation

Aa	Amino acid
Aba	4-acetamido benzoic acid
AcOH	acetic acid
AMP	antimicrobial peptide
BiFC	bimolecular fluorescence complementation
Boc	*tert*-Butyloxycarbonyl
BODIPY	borondipyrromethene
br	broad (signal) (NMR)
^{o}C	Celsius
c	concentration
Cbz	benzyloxylcarbonyl
^{13}C-NMR	Carbon-13 Nuclear Magnetic Resonance
δ	chemical shift (NMR)
d	doublet (NMR)
dd	doublet of doublet (NMR)
DCM	dichlormethane
DIC	*N,N'*-Diisopropylcarbodiimid
DIPEA	diisopropylethylamin
DMAP	4-(Dimethylamino)-pyridin
DMF	*N,N*-Dimethylformamid
DMSO	dimethyl sulfoxide
D_2O	Deuterium water
EDT	ethane-1,2-dithiol
ε (Epsilon)	molar extinction coefficient ($M^{-1}cm^{-1}$)
eq.	equivalent
ESI	Electrospray-Ionisation (MS)
F	phenylalanine
FAM	Fluorescein amidite
Fmoc	9-Fluorenylmethoxycarbonyl
FRET	Föster Resonance Energy Transfer
g	gram
h	hour, high field/upfield (NMR)
^{1}H-NMR	Proton Nuclear Magnetic Resonance
HATU	hexafluorophosphate azabenzotriazole tetramethyl uranium

HBTU	2-(1H-Benzotriazol-1-yl)-1,1,3,3-tetramethyluronium-hexafluorophosphat
Hdn	histidine-*N,N*-dinaphthalene
H_2O	water
HPLC	High Pressure Liquid Chromatography
HR-MS	High Resolution Mass Spectrometry
Hz	Hertz (s^{-1})
I	isoleucine
J	Spin-Spin-Coupling
K	Kelvin, lysine
L	liter, leucine
l	low filed/downfield (NMR)
λ (Lambda)	wavelength (nm)
LB medium	lysogeny broth medium
LTQ-FT	Linear Ion Trap and Fourier Transform (MS)
m	mass (g or mg), multiplet (NMR)
M	molar mass (g/mol)
MHz	megaherz
min	minute
mL	milliliter
mmol	millimolar
MS	mass spectrometry
n	amount of substance (mol or mmol)
NaOD	deuterated sodium hydroxide
NaOH	sodium hydroxid
NEt_3	triethylamine
nm	nanometer
NMR	Nuclear Magnetic Resonance
OD	Optical Density
Oxyma	ethyl hydroxyiminoacetate
Pbf	2,2,4,6,7-pentamethyldihydrobenzofuran-5-sulfony
pH	acidity level
ppm	parts per million
R	arginine
R_f	retention factor (TLC)

ρ (Rho)	density (g/cm^3)
RT	room temperature
RP-HPLC	Reversed Phase - High Pressure Liquid Chromatography
s	singlet (NMR)
SPPS	Solid Phase Peptide Synthesis
t	triplet (NMR)
TFA	trifluoroacetic acid
TLC	Thin-layer Chromatography
TNBS	2,4,6-Trinitrobenzene-1-sulfonic acid
UV	ultraviolet light
V	volume
W	tryptophane

2. Introduction

In this practical course, basic methods applied in chemical biology were introduced through several experiments. The organic synthesis of carboxylfluorescein and solid phase peptide synthesis (SPPS) of an antimicrobial decapeptide were performed and analysed using different methods, especially the study on spectrometric properties of fluorescein and the inhibitory effects of the peptide against selected bacteria strands.

2.1 Chemical biological theories

2.1.1 Introduction to fluorophore and biomolecule dyes

A crucial part of chemical biology is the studying of biomolecular interaction, in order to understand the structure and function of biological molecules such as DNA, proteins and many small compounds. The examination of these interactions can be seen in molecules that have been removed from their living cell, however, this might affect the chosen target with unwanted modification. On the other hand, live cell imaging offers a chance to study these molecules in their normal environment, providing not only the information about their localization and interaction, but also classifying them in specific categories for further researches. [1]

A specific method that will be discussed in this report is the application of synthetic and organic fluorescent stains to label chemical-biological compounds, making them observable by fluorescent microscopy. [2] The fluorescent visualization of biomolecules can be completed using two techniques: bimolecular fluorescence complementation (BiFC) and fluorescence resonance energy transfer (FRET). [1] BiFC is used to visualize the protein-protein interaction by forming a fluorescent complex from fluorescent fragments which are “installed” on proteins. As the proteins interact with each other, the re-formation and fluorescence of the reporter complex will showcase the protein association in living cell without being disintegrated. [3-4] Using FRET method requires an energy transfer from an excited fluorophore (donor) to another fluorophore (acceptor). [2] [4-5] FRET can be an accurate measurement of molecular level distance from 10 to 100 Å, highly efficient if the donor and acceptor are positioned within the Förster radius of 5–6 nm. [6] [7]

A fluorophore is a fluorescent chemical compound that can absorb photons in the ground state S_0, converting rapidly to fluorescence emission and vibration relaxation in the excited state S_1. This phenome can be understood using the “JABLONSKI” diagram (Fig. 1). The ground state is denoted as S_0, with S_1, S_2 and S_3 representing excited singlet states. [7] [8] When a photon is absorbed by the fluorophore, an electron will be transferred from the ground state to an excited state (blue arrow). Afterwards, the absorbed energy can be dissipated by vibration relaxation and internal conversion, indicating a change in the occurrence of the electron between

vibrational or electronic states (black, curved arrow). Another phenomenon is fluorescence, in which the electron can be lower from the first excited state to the ground state. The energy of the photon emitted in fluorescence is normally lower than the energy of the absorbed photon, which can be observed by STOKES shift (Fig. 1) – the distance between the maxima of absorption wavelength and emission wavelength. If the emitted photon has more energy than the absorbed photon, the energy difference is called an anti-STOKES shift. The electron from an excited singlet state can also change spin multiplicity to an excited triplet state, this is called an intersystem crossing (black, curves arrow). A direct transition then to the ground state is called a phosphorescence (red arrow), which is in theory a spin-forbidden transition and occurs in much slower pace than fluorescence. [9-11]

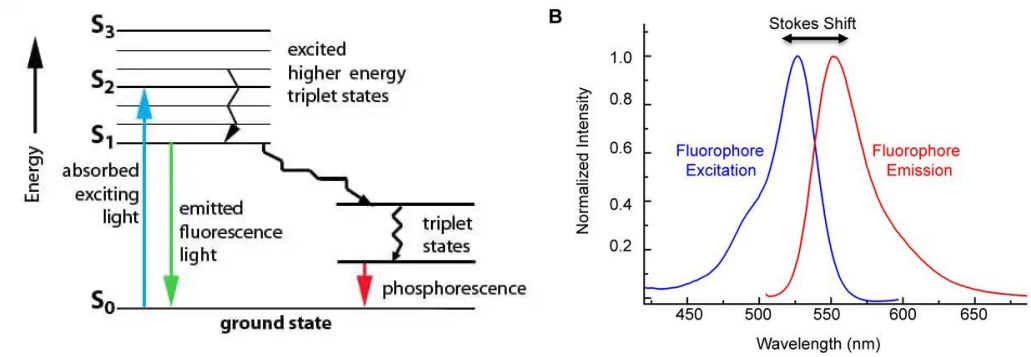

Figure 1. (left) The "JABLONSKI" diagram, including typical photophysical processes. (right) Stokes shift is measured as the distance between the absorption/excitation (blue) and emission (red) maxima. [11-12]

Aside from the typical uses in the industry like commercial fabric dyes [13] or in water quality control …,[14] fluorophores also play a crucial role in indicating and labelling biomolecules in fluorescence imaging and spectroscopy. Organic fluorophores are divided into subclasses, for examples BODIPY, cyanine dyes, fluorescein, rhodamines etc. BODIPYs are boron-coordination compounds, which are ideal for staining lipids, membranes, and other lipophilic compounds; [15] while cyanine dyes Cy3 and Cy5 are used to label nucleic acids and flow cytometry. [16] The fluorescein dye is studied in this experiment contains a tricyclic xanthene with two hydroxyl substitutional groups and a bicyclic fused lactone linked by a spiro carbon (Fig. 2). The carboxylfluorescein like 5-FAM and 6-FAM can attach its additional carboxyl group to amines through carbodiimides and *N*-hydroxysuccinimide activation. [17] In comparison to other dyes, fluorescein possesses a higher absorption, is soluble in water and has a high fluorescence quantum yield. [18]

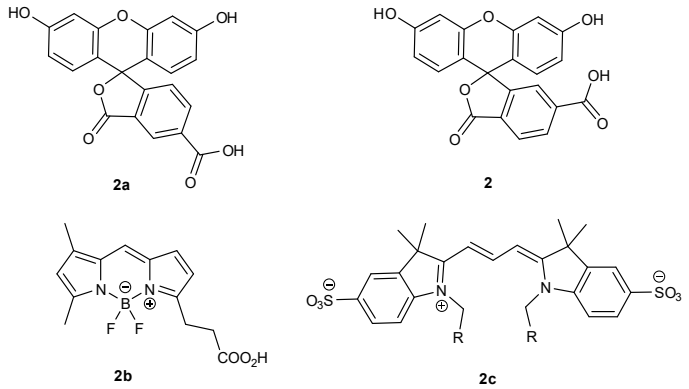

*Figure 2. Structure of organic fluorophores: (above) 5(6)-carboxylfluorescein 5-FAM **2a** and 6-FAM **2**; (below) BODIPY **2b** and cyanine dye Cy3 **2c**.*

Under different pH environments, carboxylfluorescein for example the 6-FAM, can transform from a non-fluorescent lactone form in acidic environment to a fluorescent open form in neutral to basic pH (Fig. 3). Under the excitation wavelength at 485 nm, [17] the fluorescein can be observed in different ionic forms from di-anionic to cationic.

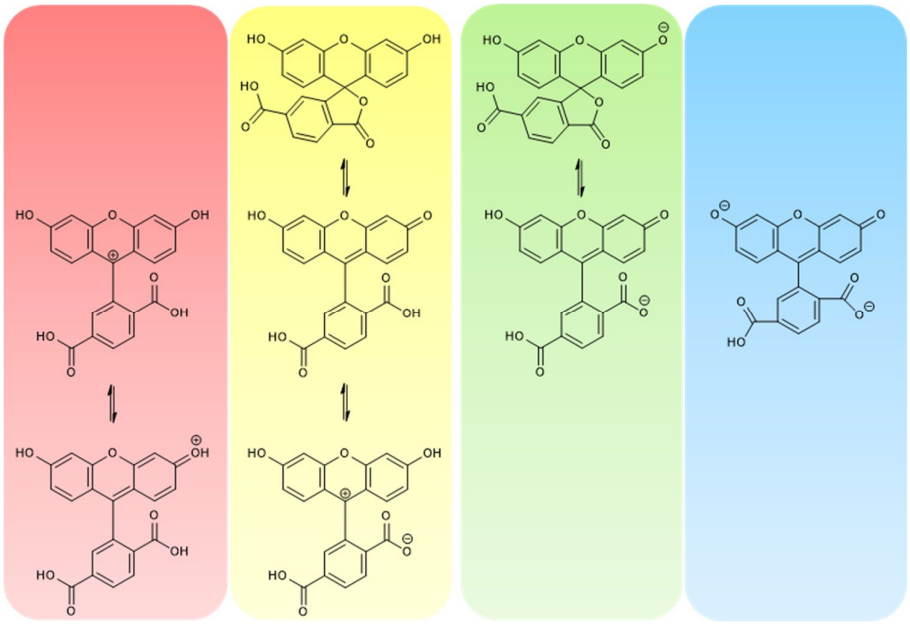

Figure 3. Ionic forms of 6-FAM in different pH domains: At neutral pH and under excitation at 485-490 nm, the most fluorescent di-anionic form (blue) is more prominent. Below pKa = 6.4 comes fluorescein in mono-anionic form (green), around lower pH from 2 to 4 it is mostly neutral (yellow) or cationic (red) at pH lower than 2 – both of these forms are less fluorescent or completely non-fluorescent. [17]

The synthesis protocol for 6-FAM **2** from 2-(2,4-dihydroxybenzoyl)terephthalic acid **1a** and resorcinol **1b** is based on the work of HAMMERSHØJ *et al.* [19] in a FRIEDEL-CRAFT acylation model (Scheme 1). The ketone oxygen atom of **1a** is protonated by methanesulfonic acid to a reactive intermediate **I**, followed by the lactonization to intermediate **III**. After the water removal

and the addition of a deprotonated resorcinol **1b**, the intermediate **V** then reacts nucleophilic on the activated vinylogous carbonyl group to form the xanthene structure **VI**. The proton exchange and water elimination, followed by the deprotonation of cyclo-diene **VII** to form aromatic ring, result in the forming of pure isomer product 6-FAM **2**.

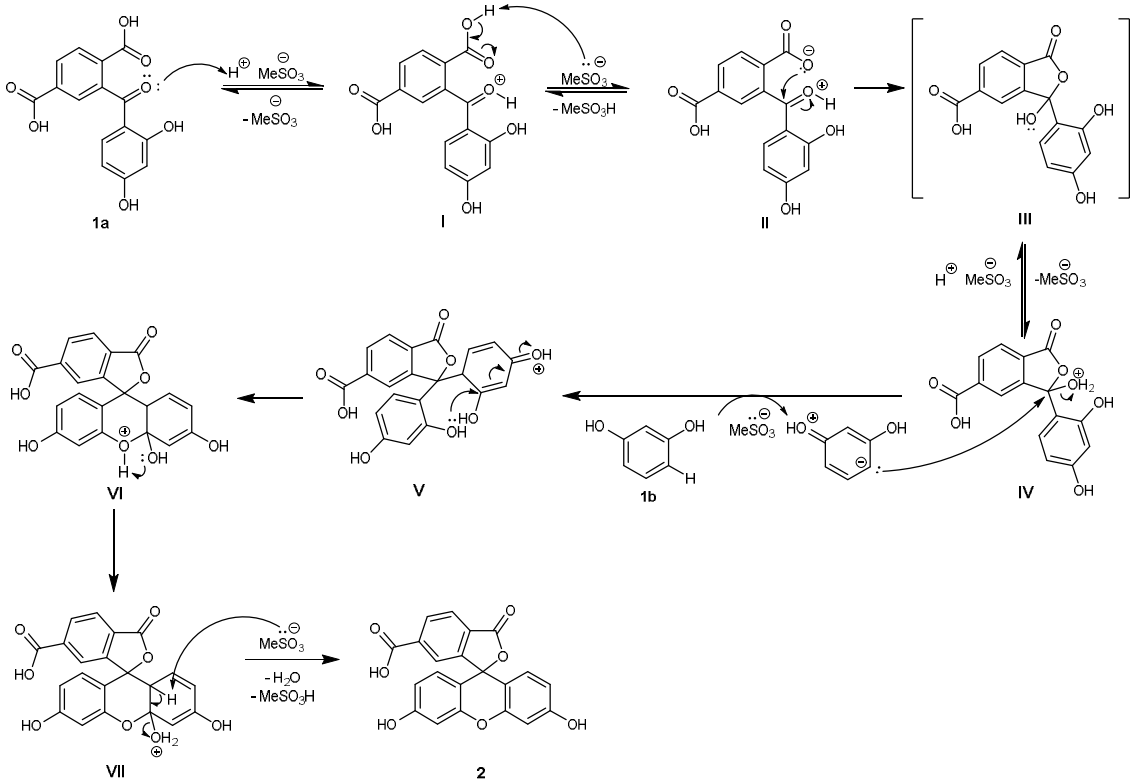

*Scheme 1. Plausible reaction mechanism of 6-FAM **2**.* [19]

2.1.2 Solid phase peptide synthesis & antimicrobial peptides

Synthesis of peptide, especially with non-natural amino acids, is an important aspect of chemical biological studies. In comparison to the classical solution-phase peptide synthesis, solid phase peptide synthesis (SPPS) has proven to be superior in terms of synthesizing short to medium-length peptides from amino acid building blocks with higher yield, more controllable stereochemistry, easy modification of the amino acids within the peptide and rapid generation of linear, macro peptides. [20] In SPPS, the first amino acid of the peptide chain is covalently bound on a solid support material (most commonly used are low cross-linked polystyrene) on its *C*-terminal, then the *N*-terminal would be deprotected to participate in the coupling with the next amino acid (Scheme 2). [21-23] The peptide chain can be easily synthesised step-by-step with the help of selective protecting group chemistry. Using basic labile *N*-terminal protected amino acids with protecting groups like fluorenylmethyloxycarbonyl (Fmoc) helps preventing self-coupling of many amino acids; while acid labile protecting groups on the side chains such

as *tert*-butylcarbonyl (Boc) and 2,2,4,6,7-pentamethyldihydrobenzofuran-5-sulfony (Pbf) [24] can be removed using tetrahydrofluoric acid (TFA) in the final cleavage.

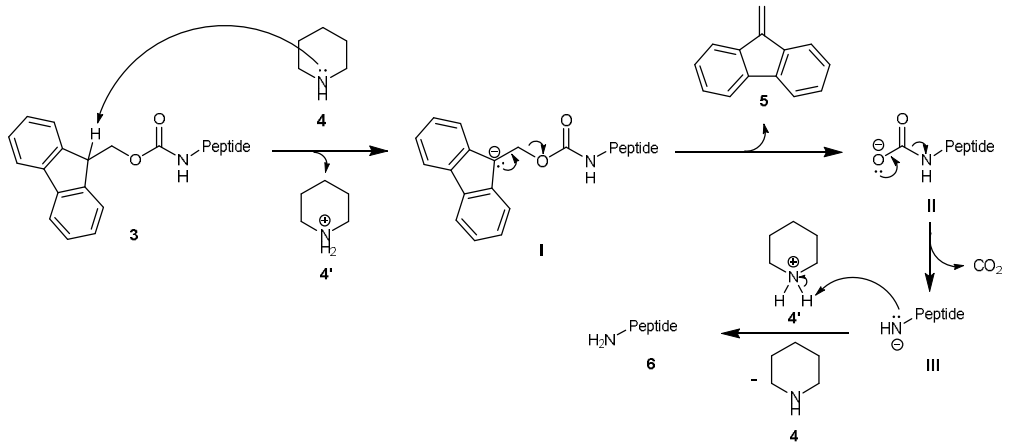

*Scheme 2. Mechanism of a Fmoc- deprotection from N-terminal of amino acid **3** with the base piperidine **4** to form the free amine of peptide **6**.*

Several resins, depending on the types of peptides, can be chosen for the SPPS: for peptide acids such as Cys, His, Gly, Pro, Met and Trp are "WANG resin" and trityl-type resin more suitable; and for peptide amides the "RINK-amide" or "SIEBER resin" are the better choice. Choosing the correct resin can prevent side reactions of peptide coupling such as enantiomerization, diketopiperazine formation or alkylation. [25]

The peptide coupling can be performed using coupling agents or agent pairs (e.g *N*,*N'*-Diisopropylcarbodiimide "DIC"/ ethyl cyanohydroxyiminoacetate "Oxyma", Hexafluorophosphate Azabenzotriazole Tetramethyl Uronium "HATU"/ *N*,*N*-Diisopropylethylamine "DIPEA", Hexafluorophosphate Benzotriazole Tetramethyl Uronium "HBTU"/ triethylamine "NEt_3"). In this course, the DIC/Oxyma method is employed since it has lower risk of explosion, efficient coupling efficiency in both manual and automated syntheses and can inhibit racemization. [26] This method needs no additional base to deprotonate the free carboxylic acid of amino acid, since DIC is already a prominent base (Scheme 3). The carboxylate **A**, forming from the deprotonation of *N*-protected amino acid **7**, attaches to the iminium-carbonyl of DIC **8** to form the *O*-acylisourea **B**. Oxyma **9** then attaches to this intermediate to form the active ester **C** after the elimination of urea side product **10**. The free *N*-terminal of the next amino acid **11** reacts to the ester **C**, resulting in the forming of the protonated amide **D**, which can be deprotonated with Oxyma carboxylate **9'** to the final peptide product **12**.

To control if the coupling is successful and there is no free amine of amino acid building block, a chemical test is often conducted, for example the "KAISER test" or 2,4,6-Trinitrobenzene-1-

sulfonic acid (TNBS). The TNBS test is employed during the course, since it doesn't involve the cyanide compound in the "KAISER test", requires no heating and the colour intensity is the same for all amino acids. [27] This test is an acid-base reaction of an indicator with the basic amino group at the *ipso* position of the aromatic ring (see attachments).

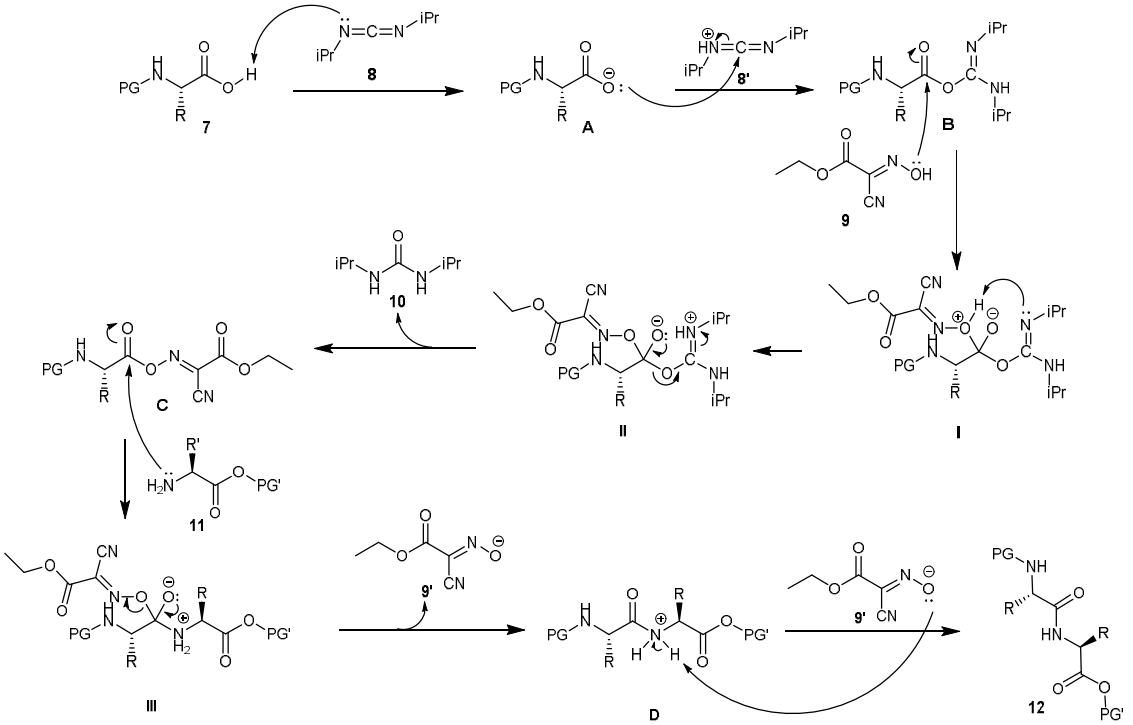

Scheme 3. Mechanism of a peptide coupling using DIC/Oxyma.

In this course an antimicrobial peptide (AMP) would be synthesized using SPPS methodology. An antimicrobial peptide is a small peptide, usually has 10–60 amino acid residues and is often charged (cationic or anionic). AMPs have a wide range of inhibitory effects against bacteria, fungi, parasites and viruses; therefore, they are also can be classified based on the target that they can inhibit. Other classification can be made based on origins (mammals, plants….), dominating amino acid in their sequence (glycine, tryptophan, proline, arginine…) or structure (*α* helix, *β* sheet or linear). [28] An important class are Arg- and Trp-rich peptides: The hydrophobic Trp interacts well with the interfacial region of lipid bilayers, while the cationic Arg residues prefers to attach to anionic components of the bacterial membrane. [28-29] These two amino acid residues can participate in cation–*π* interactions, therefore enhancing peptide–membrane interactions. Trp sidechains can also facilitate the solvation of folded proteins, where they contribute by maintaining native and nonnative hydrophobic contacts. [30]

2.1.3 Bioassay – Hemmhof test and bacteria's growth curve

The Gramm negative bacterium *Escherichia coli* (*E. coli*) is used as a target cell since it is a well-studied group of bacteria (prokaryotic organisms), easily manageable and more simply structured than eukaryotic organisms. *E. coli* is a rod-shaped, approx. 2.4 µm long Enterobacter, which is found in the intestines of animals. [31] It can be cultured at 37°C in LB medium, replicating DNA every 20 minutes – this property is important for fast and exponential replication of bacterial cells, as well as the cloning of genetic material. [32] *Bacillus subtilis* (*B. subtilis*), a well-studied example for gram-positive bacteria, is an interesting subject for many researches for its ability to produce small metabolites and enzymes, which are considered to be an evolutionary advantage. [33] This bacterium has notable physiological characteristics, highly adaptable metabolism and fast-growing, which makes it not only easy to cultivate but also to genetic modify. [33-34] The difference between these two types of bacteria lies within the construction of its membrane: Gram-negative bacteria have a thinner peptidoglycan cell wall, which is surrounded by an outer lipopolysaccharide membrane. [34-35] This outer membrane works as an effective permeability barrier against external agents like antibiotics, but can be targeted by other antibacterial agents such as polycations and chelators. [36] Gram-positive bacteria have thicker layers of peptidoglycan than Gram-negatives, however, they don't possess the outer membrane (Fig. 4). [34-35]

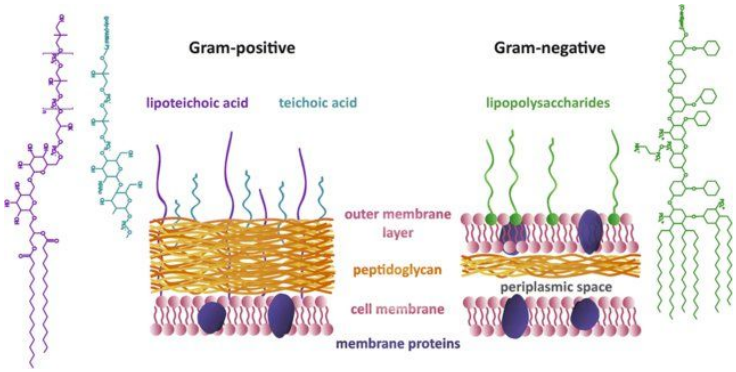

Figure 4. Simplified membrane structure of Gram positive (left) and Gram negative (right). [37]

Therefore, the value of bioassays on these two types of bacteria is that they can directly estimate the activity of bioactive substances, providing information about the potency of biological products. [38] In this course, the inhibition assay (Hemmhof test) and bacteria growth curve would be performed as examples. The Hemmhof test is a method to assess the ability of antimicrobial compounds to inhibit the growth of a specific bacterium. After culturing the bacteria overnight, it is then being spread on agar plate. The test inhibitor-producing compounds are placed on the agar surface and incubating again. After incubation, the proficiency of inhibition can be measured quantitatively through the size of the inhibition zone of clearing around the compound, and qualitatively by the clarity of the zone. [39] The study on

bacteria growth curve can be illustrated by four-phase pattern: the lag phase where bacteria first introduce to the nutritious environment, the log phase where the bacteria population increases exponentially, the stationary phase where the numbers of living and dead cell are relatively equal and the dead phase is when bacteria stop dividing and the number of dead cells exceeds the living. [40]

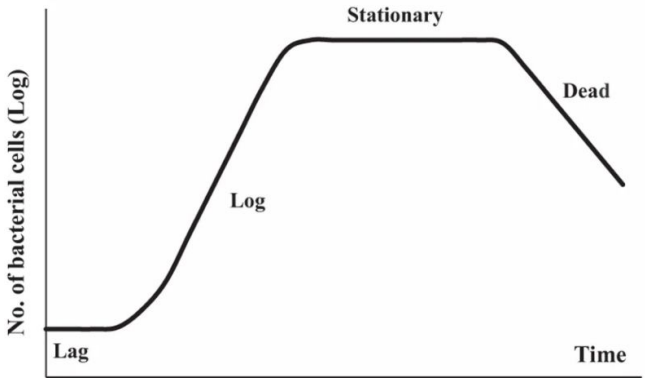

Figure 5. Graphic demonstration of a bacterial growth curve. [40]

2.2 Task summary

In this practical course, the organic synthesis of 6-FAM and SPPS of an antimicrobial decapeptide Aba-K-Hdn-RR-Hdn-IRWL-$CONH_2$ (PCB1-2) were performed. The dye was then analysed using chemical analytical methods, as well as pH dependent spectroscopy to show the sensitive structure conformation in different pH environment. The peptide was studied under similar methods and in bioassays, showing the inhibitory effects against *E. coli* and *B. subtilis*.

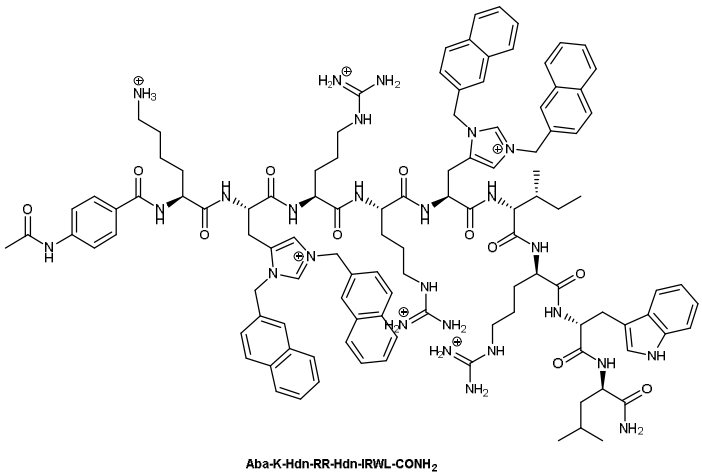

Figure 6. Molecule structure of decapeptide PCB1-2 Aba-K-Hdn-RR-Hdn-IRWL-$CONH_2$.

3. Results

All steps were prepared after script [41] and modified when needed. See more in supporting information.

*3.1 Synthesis of 6-Carboxylfluorescein 6-FAM **2***

The reaction protocol was proceeded according to the work of HAMMERSHØJ *et al.* [19] and modified when needed. The reaction was control using TLC method (10% MeOH in DCM) before and after workup. The final product was analysed by NMR using 50.0 µL of 1 mM NaOD in 0.6 mL D_2O. This experiment has to be repeated, since the first trial's yield was only around 10% and therefore not enough for a ^{13}C-NMR measurement. The second trial was proven to be more successful with a yield of 69%, which was still relatively smaller than the theoretical yield of 98%. [19] All precipitation steps and filtration were proceeded with ice-cooled media (NaOH, HCl, water…) to increase the precipitation rate of the product. By controlling the TLC (R_f before workup: 0.3; R_f after workup: 0.24), the side product and possible leftover resorcinol were already eliminated. This was again proven with the NMR spectra, however, there were signals of small, unknown particles detected in ^{1}H-NMR.

The pH dependence of spectroscopic properties from two compounds 6-FAM **2** and 6-carboxynaphthafluorescein (6-Naph) **2d** was proven using a arrange of different pH (pH = 1, 3, 5, 7, 9, 10) buffer solution, prepared after the protocol of GOMORI. [42] The absorbance of these two fluorescein was measured from 200 to 600 nm and plotted from 350 to 600 nm (Fig. 6). The high absorbance maxima of the fluoresceine in different pH environment indicate that the opened cationic form at pH = 1 at ~440 nm and di-anionic forms at neutral and basic pH at ~490 nm have a more conjugated system than the lactone neutral form (Fig. 3). This result is similar to the non-substitution fluorescein from the work of F. LE GUERN. [17] The conjugated system has a smaller HOMO-LUMO gap, therefore the energy involved in shifting the electrons in the system is smaller, resulting in a longer wavelength. [17]

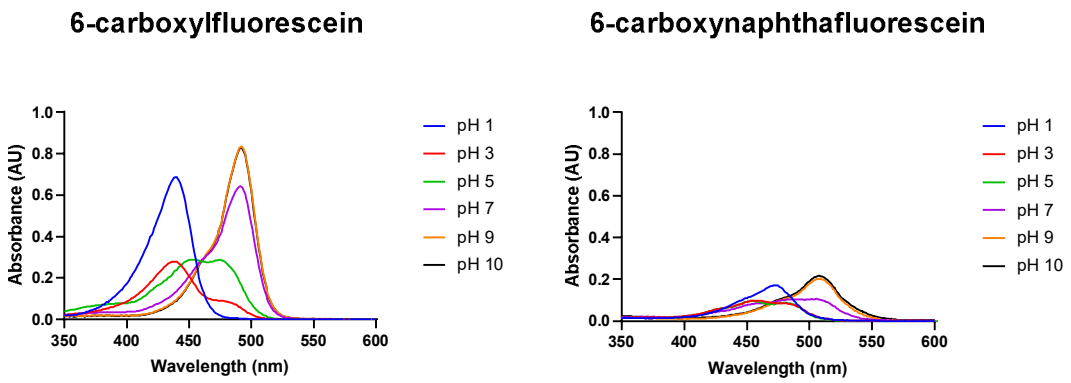

*Figure 6. Absorbance spectrum of 6-FAM **2** (left) and 6-Naph **2d** (right) at wavelengths from 350 nm to 600 nm in different buffer with pH values at 1, 3, 5, 7, 9 and 10.*

The emission was measured from 495 to 750 nm and plotted from 500 to 650 nm (Fig. 7). The high maxima of fluorescence intensity at neutral and basic pH (7, 9, 10) indicate that these compounds are non-fluorescent in acidic environment. A comparison between 6-FAM **2** and

6-Naph **2d** also indicates the potency of fluorescence regarding the conjugated system – while 6-Naph **2d** has a slightly larger conjugated xanthene structure, its absorbance and fluorescence properties are much less effective than 6-FAM **2**. It could be interpreted that the pH dependency was influenced by different residues of the conjugated chain (Fig. 8), therefore the maximum of absorbance and fluorescence of 6-Naph **2d** is further shifted to longer wavelengths. [43]

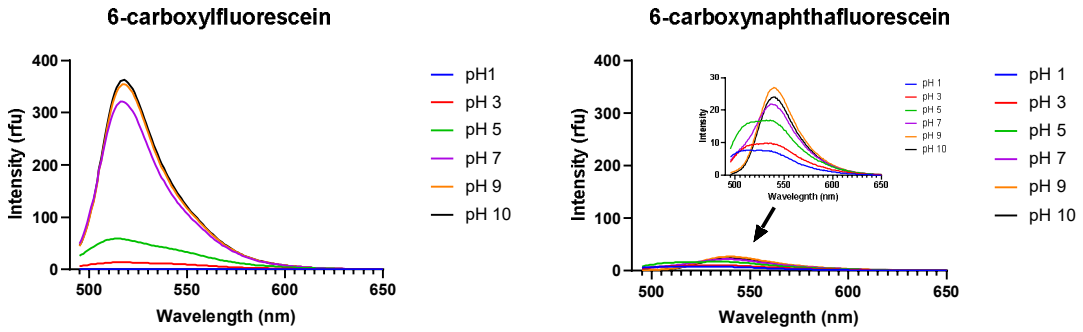

*Figure 7. Fluorescence spectrum of 6-FAM **2** (left) and 6-Naph **2d** (right) at wavelengths from 490 nm to 650 nm in different buffer with pH values at 1, 3, 5, 7, 9 and 10.*

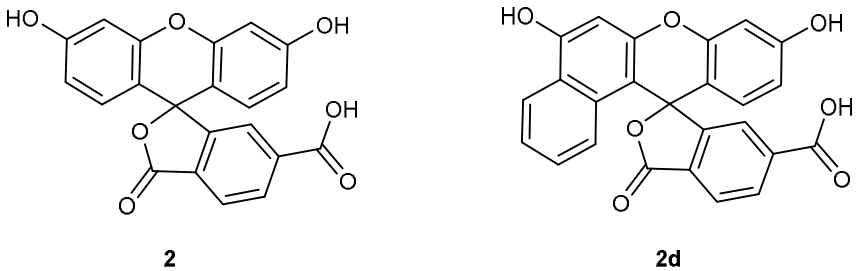

2 **2d**

*Figure 8. Structure of 6-carboxyfluorescein **2** (left) and 6-carboxylnaphthafluorescein **2d** (right).*

3.2 Solid phase peptide synthesis (SPPS)

After the SPPS, the crude peptide was then precipitated in Et_2O and further purified using HPLC-MS method. After the two purification steps, the decapeptide PCB1-2 with the sequence Aba-K-Hdn-RR-Hdn-IRWL-$CONH_2$ was then analysed using HLPC-MS and HR-MS. From the HPLC-MS spectra, the different masse per charge (m/z) of the peptide PCB1-2 (MW = 2024.6 g/mol) were detected, along with several TFA adducts and other unknown fragments (Fig. 9–12). It also might contain the Boc-protected Lys (Fig. 10) and the Pbf-protected Hdn (Fig. 12) side products. From the HR-MS, the most abundant peak was the one of +3-charge state (see supporting information).

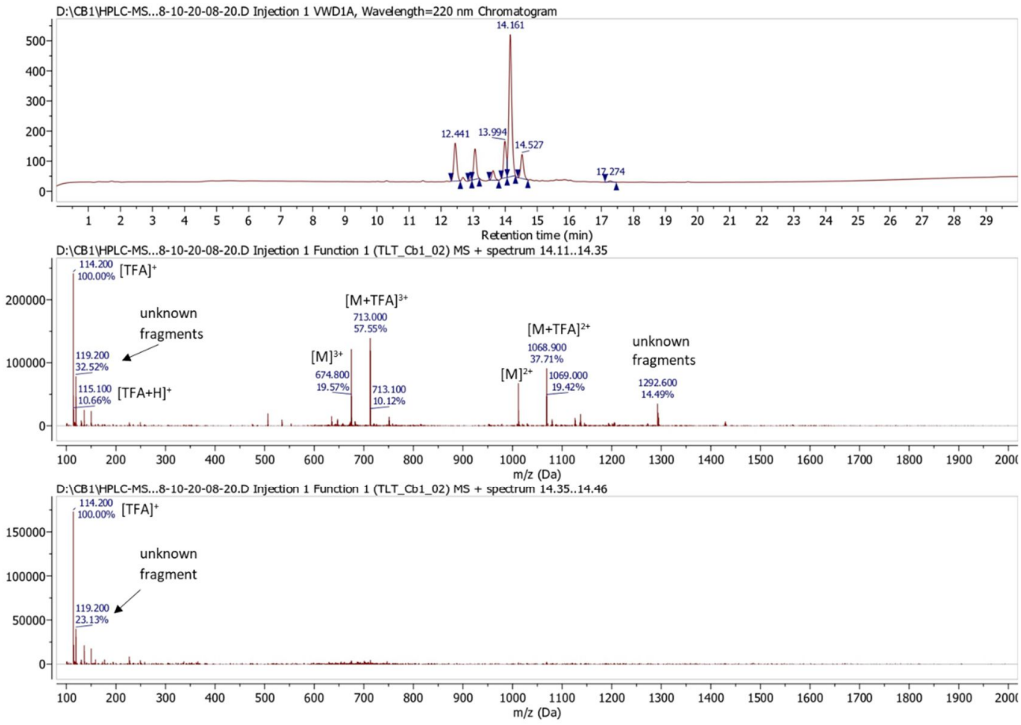

Figure 9. (above) Full HPLC-MS spectrum, (below) at R_t 14.16 minutes) spectrum at 220 nm from crude peptide PCB1-2 before purification, in gradient of 35%-75% MeCN to H_2O.

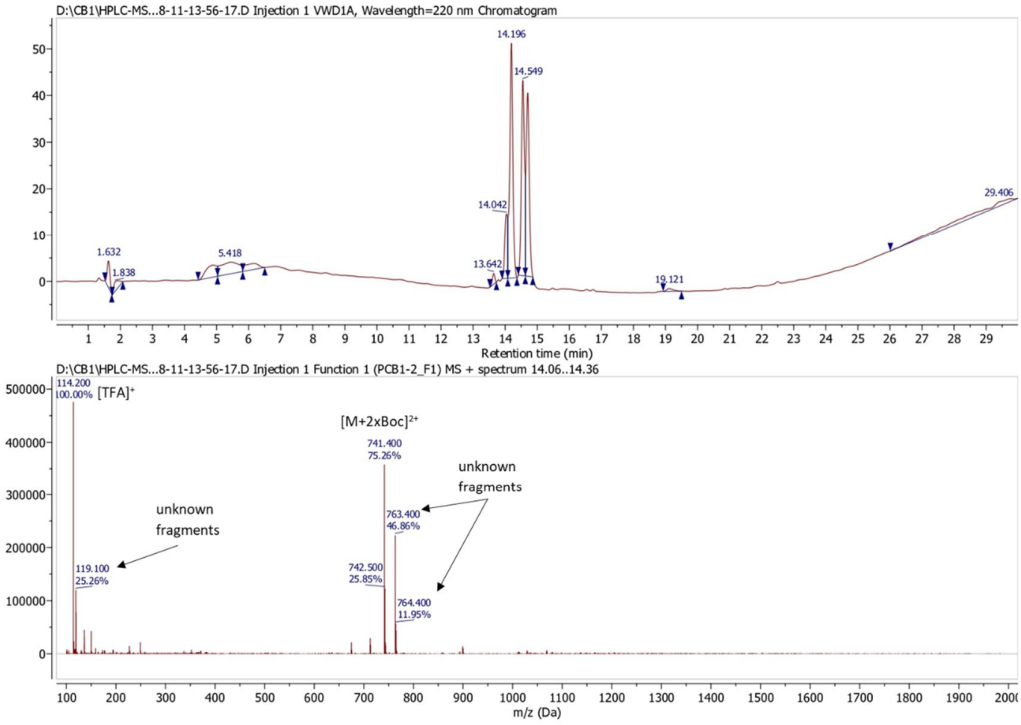

Figure 10. (above) Full HPLC-MS spectrum, (below) at R_t 14.19 minutes spectrum at 220 nm from peptide PCB1-2 after 1st purification, fraction F1, in gradient of 5% to 95% TFA/MeCN to H_2O.

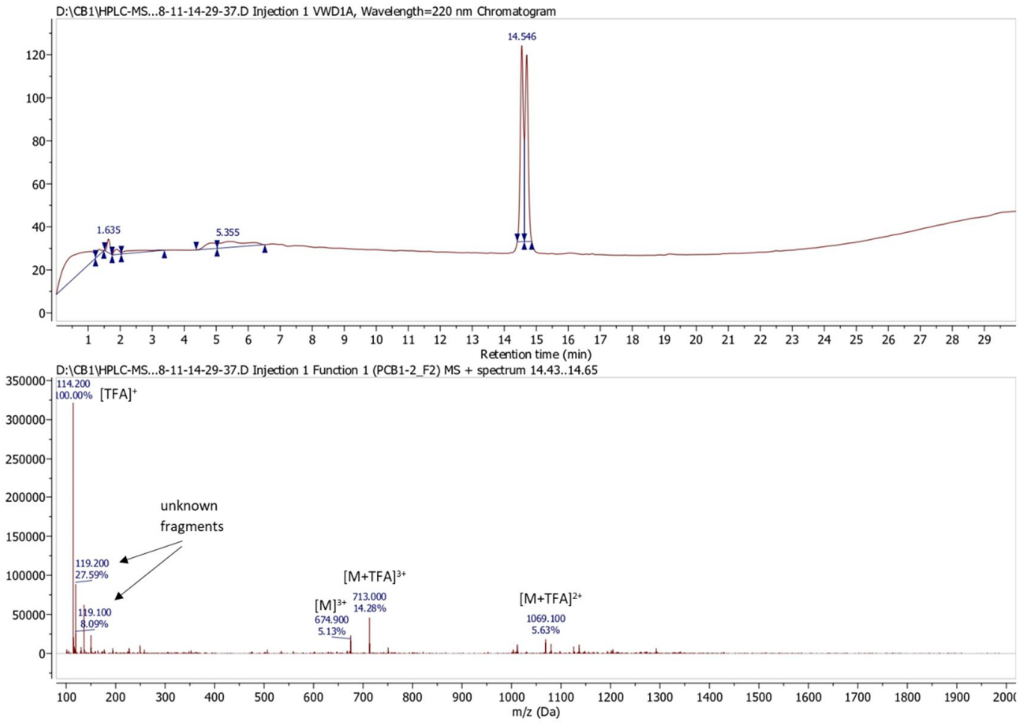

Figure 11. (above) Full HPLC-MS spectrum, (below) at R_t 14.54 minutes spectrum at 220 nm from peptide PCB1-2 after 1st purification, fraction F2, in gradient of 5% to 95% TFA/MeCN to H_2O.

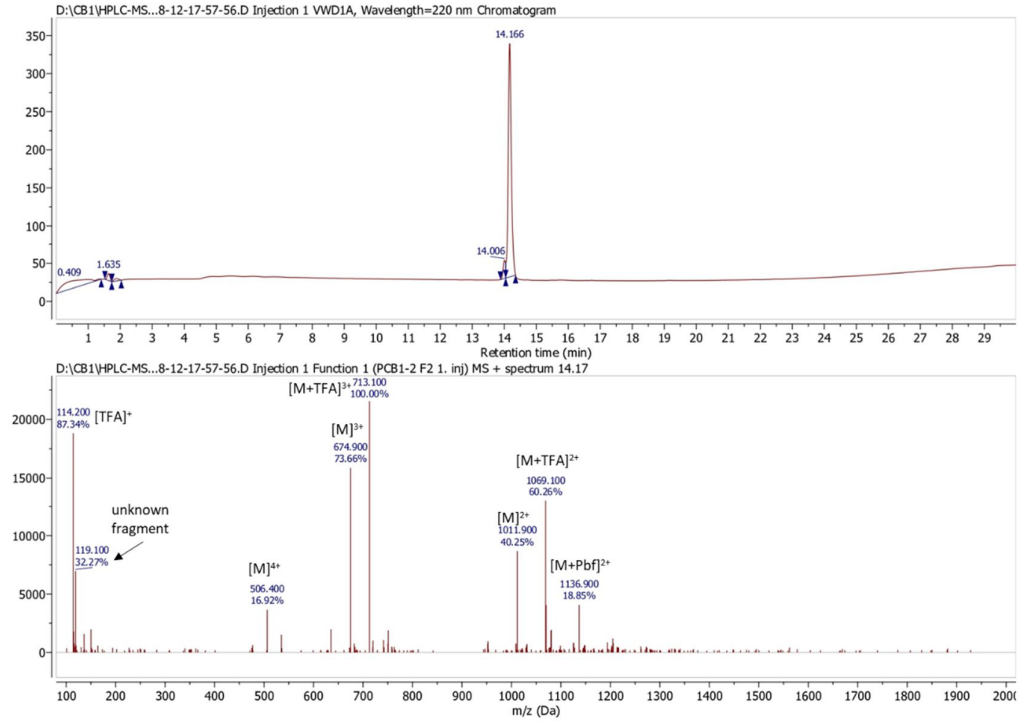

Figure 12. (above) Full HPLC-MS spectrum, (below) at R_t 14 minutes spectrum at 220 nm from peptide PCB1-2 after 2nd purification, fraction F2, in gradient of 5% to 95% TFA/MeCN to H_2O.

From the second purification, only the second fraction was pure enough to be used in the bioassays. Since there were several fractions containing contamination, the yield decreased to 4.5% from the second fraction after re-purification.

3.3 Bioassay – Hemmhof Test

The preparation of antibiotics for the Hemmhof test was similar to script. [41] After overnight incubation, the diameter of each inhibition zone including the filter paper was measured (Tab. 1). These antibiotics worked better against the Gram-negative *E. coli* species than *B. subtilis*. On the agar plate of *E. coli*, the inhibition zones were less clear; it could be because the bacteria haven't been fully dried before incubation overnight. On the plate of *B. subtilis*, the zones were uneven spread, since the distribution of the bacteria medium was not even (Fig. 13).

Table 1. Measurement of Hemmhof parameter after overnight incubation.

	Diameter of Hemmhof/cm (including filter paper)	
Antibiotics	***E. coli***	***B. subtilis***
Kanamycinsulfat **[1]**	2.0	1.6
Ciprofloxacin **[2]**	3.2	2.0
Tetracyclinehydrochlorid **[3]**	1.4	1.0
Chloraphenicol **[4]**	0.4	0.4
Polymyxin B sulfat **[5]**	1.5	0.5
Negative control (0.01 M HCl) **[6]**	0	0

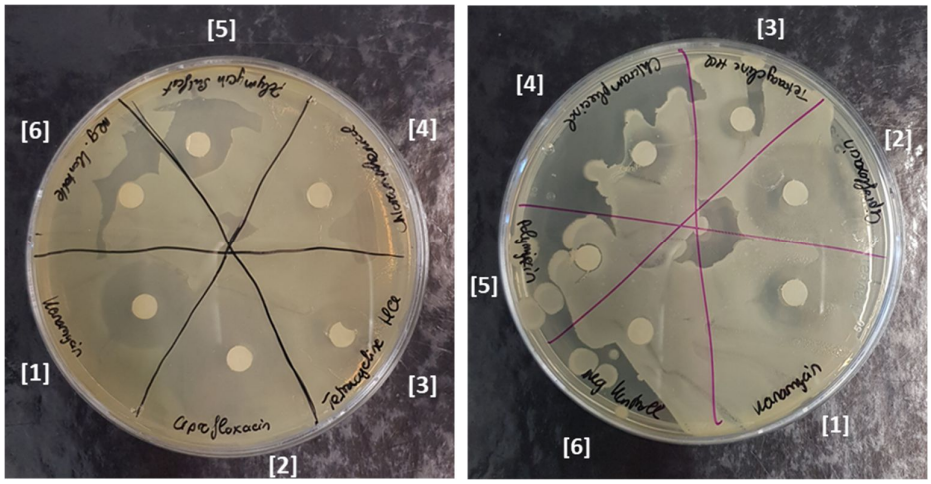

Figure 13. Agar plates with E. coli (left) and B. subtilis (right) after incubation overnight. The numbering of each portion represented each antibiotic or negative control (0.01 M HCl).

3.4 Bioassay – Growth Curve

Since the Hemmhof test shows only limited assessment of the antimicrobial effect of antibiotics on bacteria, the growth curve inhibition assay can be employed to demonstrate a detailed comparison of the antimicrobial effects of different compounds these two types of bacteria with a more exact result regarding the inhibition time and antimicrobial potency. In this experiment, an array of bacteria control (only bacteria and nutrient medium) and solvent control (0.01 M HCl) can be compared to the same bacteria strand in antimicrobial peptide concentrations. The inhibitory effect of three peptides PCB1-4, PCB1-2 and P14 were tested.

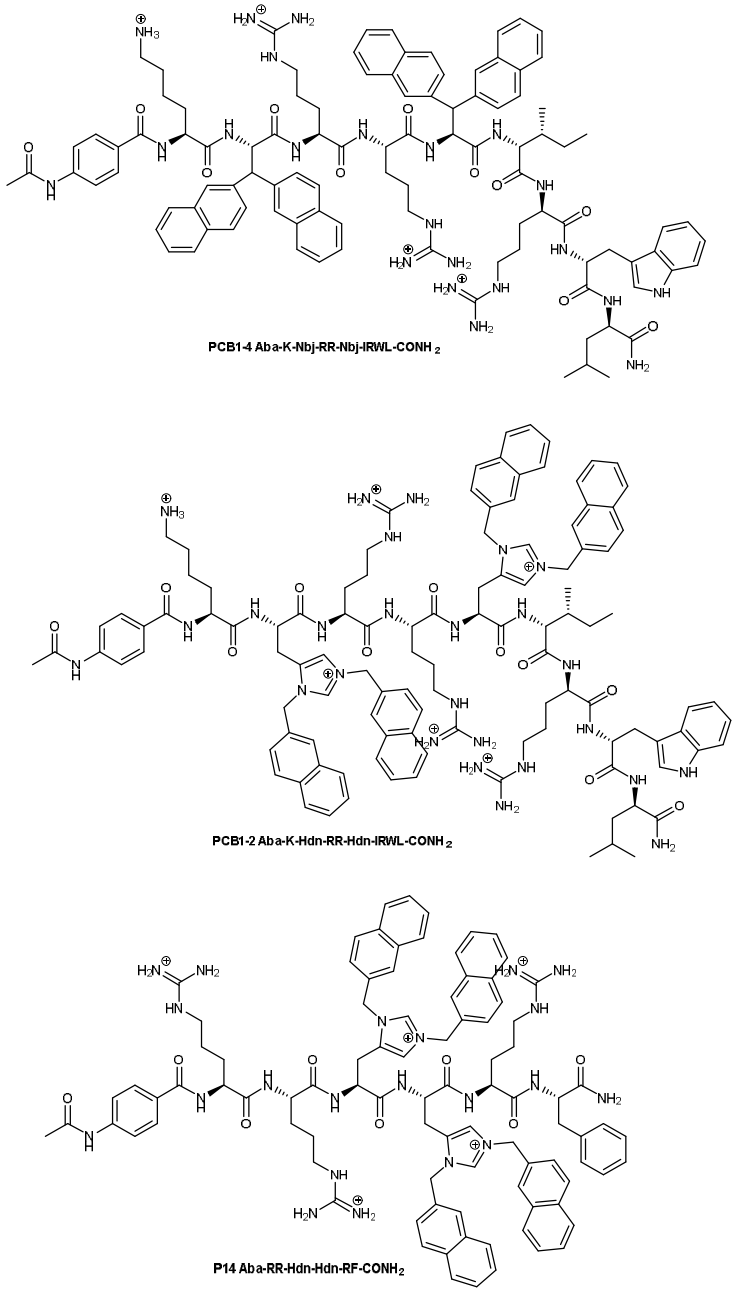

Figure 14. Molecular structure of PCB1-4, PCB-2 and P14 with their relative sequence.

The characteristic lag and log phase of each growth curve were measured by an OD_{600} intensity plate reader at 600 nm, 37°C (Fig. 15). In comparison to the bacteria and solvent controls, the growth curves of *E. coli* bacteria in different peptide concentration showed a notable delay – the three AMPs have a slight growth inhibitory but not completely bactericidal effect. On the other hand, they can significantly inhibit the growth of *B. subtilis*, with an exceptional effect in P14 and PCB1-2 peptide concentrations of 5 and 10 µM. *E. coli* was not fully inhibited by the peptides, which could happen due to the less permeable outer membrane of Gram-negative bacteria. Since the *B. subtilis* also grows faster (the growth curve is steeper), it can also be argued that the faster bacteria grow, the more they can interact with living medium including these peptides.

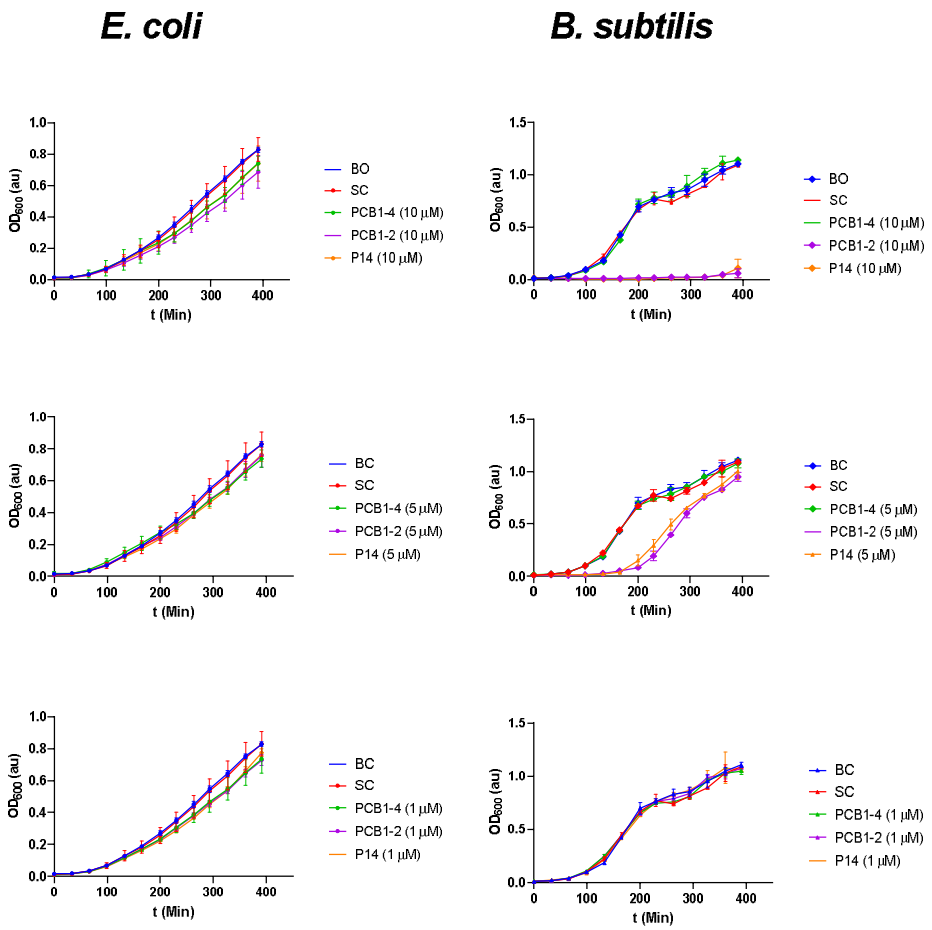

Figure 15. Growth curves of two bacteria types E. coli (left) and B. subtilis (right) in presence of antimicrobial peptides PCB1-4, PCB1-2 and P14. The inhibiting effect was compared in different peptide concentrations (10, 5 and 1 µM).

The structure of these three peptides can also be considered to be a factor for the inhibitory effect: the more cationic charged a peptide is (PCB1-2 and P14), the more likely that it can penetrate the cell membrane by building salt-bridge with the negatively charged components of the microbial membrane. [28] On the other hand, the Aba protecting group at the *N*-terminal also contribute to the antimicrobial effect; [44] its hydrophobicity is also beneficial to the peptide insertion into the membrane. [45] Another explanation could be that the hydrophilic peptidoglycan can be penetrated by the alternating hydrophobic, aromatic and hydrophilic amino acids in a peptide sequence. [46]

4. Discussion

Overall, all experiments were successfully learnt conducted in the practical course. The yield of organic synthesis was not ideal in comparison to literature: the rerun of 6-FAM synthesis has improved the yield of the product but affected its purity in comparison to the first trial; as well as the re-purification of peptide has resulted in a much smaller amount of pure peptide for the bioassays. The bioassay of Hemmhof test showed some mistakes under sterile working condition, as well as the plotting of growth curve did not fully cover the stationary phase of bacteria activities. More practising on these experiments could be an advantage in further studies.

The Hemmhof test could be done with a small probe of antimicrobial peptide instead of antibiotics, serving as a rough estimation of its inhibitory effect. The conditions for both bioassays could also been improved to accelerate the growing of bacteria. From the growing curve bioassay, modified phenylalanine and tryptophan amino acids have proven to be as effective to inhibit Gram-positive bacteria; therefore, it is also a promising subject for further researches. Since the experiment was only conducted in groups, other peptide sequences and their antimicrobial effect could also be compared on other Gram-negative and Gram-positive bacteria.

5. References

[1] T. K. Kerppola, *Nature*, **2006**, *7*, 449–455.

[2] J. C. Stockert, A. Blázquez-Castro, *Fluorescence Microscopy in Life Sciences*, **2017**, Bentham Science Publishers.

[3] T. K. Kerppola, *Annu. Rev. Biophys.*, **2008**, *37*, 465–487.

[4] K. A. Wong KA, J. P. O'Bryan, *J. Vis. Exp.*, **2011**, *50*, 2643.

[5] R. B. Sekar, A. Periasamy, *J. Cell. Biol.*, **2003**, *160*, 5, 629–633.

[6] S. M. Müller, H. Galliardt, J. Schneider, B. G. Barisas, T. Seidel, *Front. Plant. Sci.*, **2013**, *4*, 413.

[7] B. Hochreiter, A. P. Garcia, J. A. Schmid, *Sensors*, **2015**, *15*, 26281–26314.

[8] A. Jablonski, *Nature*, **1993**, *131*, 839–840.

[9] Y. Wang, J. Lin, Q. Zhang, X. Chen, H. Luan, M. Gu, *Engineering*, **2021**, *16*, 7567.

[10] H. H. Jaffe, A.L. Miller, *J. Chem. Ed.*, **1966**, *43*, 9, 469.

[11] A. Chinen, C. Guan, J. Ferrer, S. Barnaby, T. Merkel, C. Mirkin, *Chem. Rev.*, **2015**, *115*, 19.

[12] https://gauravtiwari.org/jablonski-diagram/, accessed on **25.08.23**, 16:03.

[13] R. M. Christie, *Handbook of Textile and Industrial Dyeing*, **2011**, Woodhead Publishing, *1*, 17, 562–587.

[14] D. N. Myers, *Separation Science and Technology*, **2019**, Academic Press, *11*, 10, 219–283.

[15] https://www.thermofisher.com/de/de/home/life-science/cell-analysis/fluorophores/bodipy-fl.html, accessed on **25.08.23**, 16:06.

[16] https://www.thermofisher.com/de/de/home/life-science/cell-analysis/fluorophores/cy3-dye.html, accessed on **25.08.23**, 16:06.

[17] F. Le Guern, M. Vanessa, A. Gaucher, M. Rottman, D. Prim, *Int. J. Mol. Sci.*, **2020**, *21*, 9217.

[18] X. He, L. Hu, L. Zou, J. Zhong, H. Luo, Z. Pu, *Mater. Lett.*, **2021**, *293*,129668.

[19] P. Hammershøj, E. K. P. Kumar, P. Harris, T. L. Andresen, M. H. Clausen*, Eur. J. Org. Chem.*, **2015**, *33*, 7301–7309.

[20] S. J. Kim, S. R. McAlpine, *Molecules*, **2013**, *18*, 1, 1111–1121.

[21] F. Guillier, D. Orain, M. Bradley, *Chem. Rev.*, **2000**, *100*, 6, 2091–2158.

[22] M. Stawikowski, G. B. Fields, *Curr. Protoc. Protein. Sci.*, **2002**, *18*, 1, 3–4.

[23] R. B. Merrifield, *J. Am. Chem. Soc.*, **1963**, *85*, 14, 2149–2154.

[24] L. A. Carpino, H. Shroff, S. A. Triolo, E. M. E. Mansour, *Tetrahedron Lett.*, **1993**, *34*, 7829.

[25] https://www.sigmaaldrich.com/DE/de/technical-documents/technical-article/chemistry-and-synthesis/peptide-synthesis/linkers-fmoc-spps, accessed on **26.08.23**, 01:47.

[26] X.-T. Chen, J.-Y. Wang, Y.-N. Ma, L.-Y. Dong, S.-X. Jia, H. Yin, X.-Y. Fu, S.-S. Du, Y.-K Qi, K. Wang, *J. Pep. Sci*, **2022**, *28*, 3, e3368.

[27] W. S. Hancock, J. E. Battersby, *Anal. Biochem.*, **1976**, *71*, 1, 260–264.

[28] Y. Huan, Q. Kong, H. Mou, H. Yi, *Front. Microbiol.*, **2020**, *11*, 1–2.

[29] L. Jin, X. Bai, N. Luan, H. Yao, Z. Zhang, W. Liu, Y. Cheng, X. Yan, M. Rong, R. Lai, Q. Lu, *J. Med. Chem.*, **2016**, *59*, 5, 1791–1799.

[30] S. Barik, *Int. J. Mol. Sci.*, **2020**, *21*, 22, 8776.

[31] https://www.cdc.gov/ecoli/general/index.html, accessed on **27.08.23** at 22:26.

[32] J. Jaruszewicz-Błońska, T. Lipniacki, *BMC Syst. Biol.*, **2017**, *11*, 1, 117.

[33] Y. Su, C. Liu, H. Fang, D. Zhang, *Microb. Cell. Fact.,* **2020**, *19*, 173.

[34] J. Chen, Y. Zhu, G. Fu, Y. Song, Z. Jin, Y. Sun, D. Zhang, *J. Ind. Microbiol. Biotechnol.*, **2016**, *43*, 11, 1577–1591.

[35] T. J. Silhavy, D. Kahne, S. Walker, *Cold Spring Harb Perspect Biol.*, **2010**, *2*, 5, a000414.

[36] M. Vaara, *Microbiol Rev.*, **1992**, *56*, 3, 395–411.

[37] W. Pajerski, D. Ochońska, M. Brzychczy-Włoch, P. Indyka, M. Jarosz, M. Golda-Cepa, Z. Sojka, A. Kotarba, Andrzej, *J. Nanopart. Res.*, **2019**, *21*, 186.

[38] R. Thorpe, M. Wadhwa, A. Mire-Sluis, *Dev. Biol. Stand.*, **1997**, *91*, 79–88.

[39] J. C. Moran, E. L. Crank, H. A. Ghabban, M. J. Horsburgh, *J. Vis. Exp.*, **2016**, *115*, 54437.

[40] L. Wang, D. Fan, W. Chen, E. M. Terentjev, *Sci. Rep.*, **2015**, *5*, 15159.

[41] V. T. Trinh, V. Viereckt, *Script of Practical Course CB1- Chemical Biology SS2023*, Phillips University Marburg, Faculty Chemistry (FB 15), **2023**, 2, 8–9.

[42] G. Gomori, *Meth. Enzymol.*, **1955**, *1*,138–146.

[43] V. Wycisk, K. Achazi, P. Hillmann, O. Hirsch, C. Kuehne, J. Dernedde, R. Haag, K. Licha, *ACS Omega*, **2016**, *1*, 5, 808–817.

[44] G. M. Brown, *J. Biol. Chem.*, **1962**, *237*, 2, 536–540.

[45] L. Liu, L. Zhao, L. Liu, S. Yue, J. Wang, Z. Cao, *Langmuir*, **2020**, *36*, 50, 15189–15462.

[46] C. Tanford, *Science*, **1978**, *200*, 4345, 1012–1018.

6. Attachment:

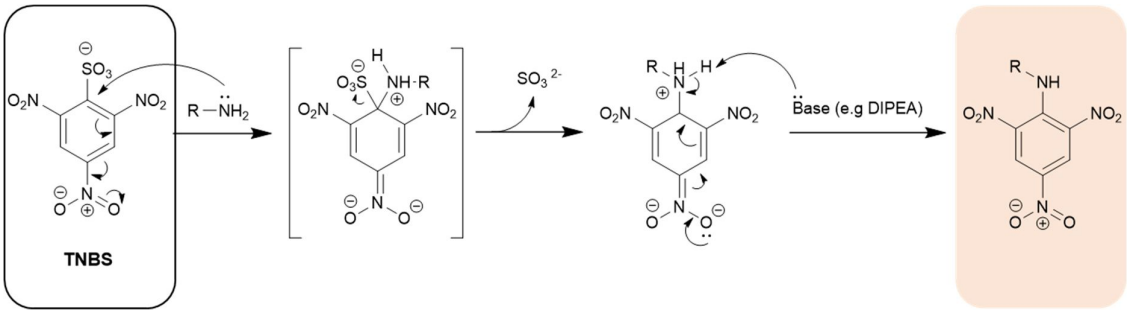

Scheme 4. Mechanism of a positive TNBS test with free amine groups of amino acid, which turns the colourless beads to red-orange.